Wire perturbations in the Saffman-Taylor problem: Pattern selection of asymmetric fingers

D. C. Hong
Department of Physics, Emory University, Atlanta, Georgia 30322
*and Department of Physics, Building 16, Lehigh University, Bethlehem, PA 18015**
(Received 9 June 1988)

Solvability conditions are derived for the asymmetric Saffman-Taylor finger. In the absence of surface tension the solution contains two free parameters λ and y_0, where λ is the dimensionless finger width and y_0 is the degree of asymmetry. In the presence of surface tension, it is shown that solvability conditions are not satisfied, signaling the appearance of a cusp on the finger boundary. The mismatch angle, $\Delta\theta$, due to this cusp is shown to be concave. An earlier postulate made in connection with the wire experiment is clarified here, which states that $\Delta\theta$ mainly depends on the tangential slope of the finger profile. The remaining portion of this paper is devoted to understanding recent experiments by G. Zocchi and co-workers and M. Rabaud and co-workers [Phys. Rev. A **35**, 1894 (1987); **37**, 935 (1988)], where fingers were perturbed by wires. Assuming the contact angle created by the wire to be concave, we first show within linear approximation that, for $y_0 \ll 1$, the absolute magnitudes of the mismatch angles created by the wire and the bubble at the center are the same, establishing that all the results obtained by the bubble perturbations can be carried over to a wire experiment. We then present a theoretical prediction for δ, the distance between the tip of the asymmetric finger and the wire at the center, as a function of external parameters. In the limit of small surface tension, the results are in fair agreement with the available data.

I. INTRODUCTION

In a previous paper[1] the author proposed a model for the recent experiment performed by Zocchi, Shaw, Libchaber, and Kadanoff.[2] They placed two wires symmetrically along the center of a Hele-Shaw cell and observed a transition from a symmetric to an asymmetric finger shape as the pushing velocity was increased. The model assumed that the wire creates a negative opening angle at the contact point, and the analysis was carried out for the symmetric finger. This analysis, together with an earlier investigation on Couder's finger[3] with a bubble at the tip,[4] has advanced our understanding of two fundamental static external perturbations on the Saffman-Taylor finger:[5] bubble perturbation[4] and wire perturbation,[1] creating positive and negative opening angles at the contact point, respectively. The dynamics[6] and stability of the fingers[7] with wire and bubble perturbations, however, are still open questions. The selection mechanism for the steady-state asymmetric Saffman-Taylor finger[8] has not yet been fully investigated, either.

For the symmetric finger, the selection mechanism is now completely understood.[9,10] In the absence of surface tension, the experimentally measurable quantity λ, defined as the dimensionless width of the finger, enters the problem as an undetermined variable[5] and thus a continuous family of solutions exists. The surface tension breaks this continuous family into a discrete set and only one of them is dynamically stable and selected.

For the asymmetric finger, however, there is an additional parameter y_0 which measures the degree of asymmetry of the finger. Now the natural question to ask is whether surface tension is enough to break the continuous family of solutions and select a unique asymmetric-finger state. Does a two-parameter continuous family of solutions break into the discrete set? Or does the family of solutions simply cease to exist with surface tension? To date, a steady-state asymmetric finger has not been observed without an external perturbation such as a wire. It appears that the zero-surface-tension solutions cease to exist in the presence of surface tension. Recently, Tanveer[11] has shown that the two-parameter family of solutions disappears when surface tension is turned on. By assuming that the finger boundary is smooth, he has written down the solvability condition and has shown that it is satisfied only when the asymmetry parameter $y_0=0$. His solvability condition correctly yields the predicted $\frac{2}{3}$ power law[9] for the symmetric finger between λ and the small parameter ν, which will be defined later. The mathematical analysis, however, does not seem to give a clear physical picture of what is actually happening to the zero-surface-tension solution when surface tension is turned on. The present analysis is based on Tanveer's linearized equation of motion for the finger profile but several new results will be presented in this paper. First, the solvability conditions derived in this paper have a direct physical meaning and are different from those obtained by Tanveer: surface tension creates a concave cusp for the asymmetric finger at the center of the cell. Second, the result can be directly applied to the wire experiments of Zocchi *et al.* and Rabaud, Couder, and Gerard.[2]

The outline of this paper is as follows. In Sec. II it will be shown that for an asymmetric finger, two solvability conditions should be simultaneously satisfied for a given surface tension. The surface tension alone is not enough to satisfy these two solvability conditions. Since the solvability conditions are not satisfied, a cusp will appear at the finger boundary in the presence of surface tension. We will show in Sec. III that the cusp is concave (or by an earlier definition has a negative mismatch angle) and propose a model for the wire experiments performed by

Zocchi *et al.* and Rabaud *et al.* by assuming that the wire creates a concave cusp at the contact point. The previously obtained results for the Saffman-Taylor finger[1] are confirmed by a new derivation and new theoretical predictions are presented and compared with experimental results.

II. SOLVABILITY CONDITIONS FOR AN ASYMMETRIC SAFFMAN-TAYLOR FINGER IN THE PRESENCE OF SURFACE TENSION

Consider the two-fluid motion in a two-dimensional Hele-Shaw cell. The Hele-Shaw cell is made of two infinitely long glass plates of width W, which are vertically a distance $b \ll W$ apart. The side walls of the cell are blocked and the motion of the fluid is confined along the x direction (Fig. 1). Instability sets in when a less viscous fluid pushes a more viscous one. This instability grows and after a transient period, one single steady finger with a well-defined finger width develops inside the cell. The governing equations of motion for the finger in the cell are very simple. The velocity v satisfies Darcy's law everywhere inside the cell:

$$v = -\frac{b^2}{12\mu}\nabla P = \nabla\phi \ , \tag{2.1}$$

where P is the pressure, μ is the fluid viscosity, and ϕ is the velocity potential. The fluid is incompressible and the pressure P and ϕ will satisfy the Laplace equation:

$$\nabla^2\phi = 0 \ . \tag{2.2}$$

Two boundary conditions must be satisfied at the finger boundary:

$$v_n = \frac{\partial\phi}{\partial n} \ , \tag{2.3}$$

where v_n is the normal velocity of the finger surface and the derivative is taken along the normal direction, and

$$\phi_s = \frac{\gamma b^2 \kappa}{12\mu} \ , \tag{2.4}$$

where ϕ_s is the value of ϕ at the surface and κ is the curvature. The viscosity of the pushing fluid is simply set to zero. At the side walls, the normal velocity of the fluid vanishes. In the absence of surface tension γ, the above equation was solved by Saffman and Tayor:[5] they obtained a two-parameter family of asymmetric solutions.

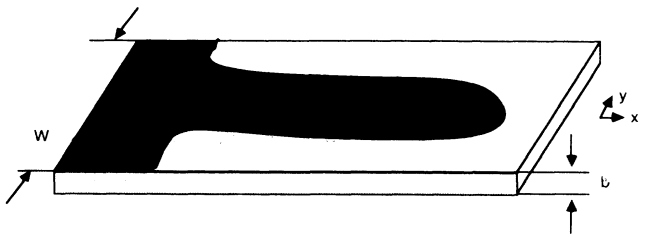

FIG. 1. Schematic picture of the Hele-Shaw cell.

For later purposes, we will write down their solution:

$$\zeta_0(y) = \frac{2}{\pi}(1-\lambda)\ln\left[\cos\left[\frac{\pi(y-y_0)}{2\lambda}\right]\right] + \frac{2y_0}{\pi}\ln\left[\tan\left[\frac{\pi}{4}+\frac{\pi}{4\lambda}(y-y_0)\right]\right] \ , \tag{2.5}$$

where $\zeta_0(y)$ is the zero surface tension finger profile, λ is the dimensionless width of the finger, and y_0 is the degree of asymmetry ranging from 0 to 1.

What happens to this zero-surface-tension solution when surface tension is turned on? In order to answer this question, we now follow the standard procedures of solvability theory established recently for pattern selection in nonequilibrium dissipative systems: Write down the linear integro-differential equation for the shape correction and look for a solvability condition by constructing the adjoint operator. After straightforward algebra, we now obtain the following equation for shape correction from Tanveer's equation of motion [Eq. (20) in Ref. 11]:

$$\nu\frac{d^2\zeta_1}{d\eta^2} + \nu P_0(\eta)\frac{d^2\zeta_2}{d\eta^2} + \nu P_1(\eta)\frac{d\zeta_1}{d\eta} + \nu P_2(\eta)\frac{d\zeta_2}{d\eta} + Q(\eta)\zeta_1(\eta) = R(\eta) \ , \tag{2.6}$$

where

$$P_0(\eta) = -\eta - \frac{y_0}{\lambda}(1+\beta^2\eta^2)^{1/2} \ , \tag{2.7a}$$

$$P_1(\eta) = \frac{2}{\beta}h(\eta)\frac{P_0(\eta)}{1+P_0^2(\eta)} \ , \tag{2.7b}$$

$$P_2(\eta) = -\frac{1}{\beta}h(\eta)\frac{1-P_0^2(\eta)}{1+P_0^2(\eta)} \ , \tag{2.7c}$$

$$h(\eta) = (1+\beta^2\eta^2) + \frac{y_0}{\lambda}\beta^2\eta(1+\beta^2\eta^2)^{1/2} \ , \tag{2.7d}$$

$$Q(\eta) = 4\beta^4\frac{[1+P_0^2(\eta)]^{3/2}}{(1+\beta^2\eta^2)^2} \ , \tag{2.7e}$$

$$R(h) = -\frac{\nu\beta^2}{(1+\beta^2\eta^2)^2}[(1-\lambda)(1+\beta^2\eta^2)] + \frac{y_0}{\lambda\eta}(1+\beta^2\eta^2)^{1/2} \ , \tag{2.7f}$$

$$\zeta_2(\eta) = -\frac{1}{\pi}\int_{-\infty}^{+\infty}\frac{d\eta\,\zeta_1(\eta')}{\eta'-\eta}\frac{2\eta}{\eta'+\eta} \ , \tag{2.7g}$$

and the small parameters ν and β are defined as

$$\beta = \frac{\lambda}{1-\lambda} \ , \tag{2.8a}$$

$$\nu = \frac{b^2\gamma\pi^2}{12\mu UW^2(1-\lambda)^2} \ , \tag{2.8b}$$

$$\cot\left[\frac{\pi}{2\lambda}(y-y_0)\right] = -\beta\eta \ . \tag{2.9}$$

The next step is to construct the null eigenvectors $Z_{\pm}$

to the adjoint operators of the homogeneous part of Eq. (2.6). This is easily constructed by changing the signs in front of $P_0(\eta)$ and the $P_1(\eta)$. Following the arguments discussed in Ref. 12 and subsequently used in recent work on Saffman-Taylor problems,[1,4] we can construct an equation of motion for the two null eigenvectors $Z_\pm$:

$$\nu\frac{d^2Z_\pm}{d\eta^2}-\nu P_\pm(\eta)\frac{dZ_\pm}{d\eta}+Q_\pm(\eta)Z_\pm=0\ , \tag{2.10}$$

where

$$P_\pm(\eta)[1+iP_0(\eta)] =\frac{2\beta^2\eta}{1+\beta^2\eta^2}[1\pm iP_0(\eta)]-\frac{ih(\eta)[1\pm iP_0(\eta)]^2}{(1+\beta^2\eta^2)[1+P_0^2(\eta)]}\ , \tag{2.11}$$

$$Q_\pm(\eta)=\frac{Q(\eta)}{1\pm iP_0(\eta)}\ . \tag{2.12}$$

WKB solutions to Eq. (2.10) can be easily constructed, having the form

$$Z_\pm(\eta)=\frac{(1+\beta^2\eta^2)}{\sqrt{2}\beta}\frac{[1+iP_0(\eta)]^{3/4}}{[1+iP_0^2(\eta)]^{7/8}}\exp\left[i\frac{\Psi(\eta)}{\sqrt{\nu}}\right]\ , \tag{2.13}$$

where

$$\frac{\Psi(\eta)}{\sqrt{\nu}}=\frac{2\iota\beta^2}{\sqrt{\nu}}\int_0^\eta\frac{d\eta'[1\pm\iota P_0(\eta)]^{1/4}[1\mp iP_0(\eta)]^{3/4}}{(1+\beta^2\eta'^2)}\ . \tag{2.14}$$

Note that $Z_+(\eta)=Z_-(\eta)^*$. In order for the solvability conditions to be satisfied, $Z_\pm(\eta)$ must be orthogonal to the inhomogeneous function $R(\eta)$. Since $Z_\pm(\eta)$ as well as $R(\eta)$ are neither symmetric nor antisymmetric, the solvability function Π, defined as the inner product between $Z_+(\eta)$ and $R(\eta)$, will be complex and thus the two solvability conditions must be satisfied. We find

$$\Pi=\langle Z_+(\eta)R(\eta)\rangle=\langle Z_-(\eta)R(\eta)\rangle^* =\int_{-\infty}^{\infty}d\eta\,F(\eta)\exp\left[i\frac{\Psi(\eta)}{\sqrt{\nu}}\right] =\Pi_1-i\Pi_2\ , \tag{2.15}$$

where

$$F(\eta)=-\left[\frac{\nu\beta^2(1-\lambda)}{1+\beta^2\eta^2}\right]\left[1+\frac{y_0}{\lambda(1-\lambda)\eta}\frac{1}{(1+\beta^2\eta^2)^{1/2}}\right] \times\left[\frac{(1+\beta^2\eta^2)^{1/2}}{\sqrt{1+\iota\eta}}\right]Q^{-1/4}(\eta)\ . \tag{2.16}$$

Note that if $y_0=0$, Π_2 would be zero, and we need to satisfy only one solvability condition $\Pi_1=0$. Nonzero y_0 produces an additional term Π_2. We now use the steepest-descent methods to evaluate the integrals Π_1 and Π_2. In the presence of finite y_0, the stationary phases gain additional terms which are proportional to y_0. By setting the denominator of $\Psi(\eta)$ to zero, we find that the new stationary points $\eta_\pm$ are given by

$$\eta_\pm=\pm i\mp i\frac{y_0}{\lambda}(\beta^2-1)^{1/2}\ \text{ if } \lambda>\tfrac{1}{2} \tag{2.17a}$$

$$=\pm i\mp\frac{y_0}{\lambda}(1-\beta^2)^{1/2}\ \text{ if } \lambda<\tfrac{1}{2}\ . \tag{2.17b}$$

Note that for $\lambda>\frac{1}{2}$, the new stationary points move toward the origin along the imaginary axis, while for $\lambda<\frac{1}{2}$ they shift to the left, producing a real part. We now consider two distinct limits: $\lambda<\frac{1}{2}$ and $\lambda>\frac{1}{2}$.

(a) $\lambda<\frac{1}{2}$. In this case the branch cuts run from $\eta=\pm i$ to $\pm i\infty$. Moreover, additional branch cuts run from $\eta=\eta_\pm$ to $\eta_\pm\pm i\infty$ because the new stationary point $\eta_\pm$ moves to the left. The steepest-descent path runs from $-\infty$ to the branch point $\eta_\pm$, cutting the imaginary axis between $\pm i$ and 0, and then runs away to $\pm\infty$. The integration can be performed by expanding $\Psi(\eta)$ near $\eta=\eta_+$ for $|\eta-\eta_+|\ll y_0\ll 1$:

$$\Psi(\eta)\approx-\beta^2G(\lambda)-\frac{8}{7}\left[\frac{2}{i}\right]^{1/4}\left[\frac{\lambda^2}{1-2\lambda}\right](\eta-\eta_+)^{7/4}\ , \tag{2.18a}$$

where

$$G(\lambda)=-\frac{\Psi(\eta_+)}{\beta^2} =2\int_0^1dx\frac{(1-x)^{3/4}(1+x)^{1/4}}{1-\beta^2x^2}+i\frac{y_0}{\lambda}g(\lambda)\ , \tag{2.18b}$$

with

$$g(\lambda)=\int_0^1dx\frac{1/2+x}{(1+x)^{3/4}(1-x)^{1/4}}\frac{1}{(1-\beta^2x^2)^{1/2}}\ . \tag{2.18c}$$

The solvability condition (2.15) now can be evaluated by the steepest-descent method. We find

$$\Pi\approx\Pi_0\left[\cos\left[\frac{2y_0\beta^2g(\lambda)}{\lambda\sqrt{\nu}}\right]-i\sin\left[\frac{2y_0\beta^2g(\lambda)}{\lambda\sqrt{\nu}}\right]\right]\ , \tag{2.19}$$

where Π_0 is the solvability function for $y_0=0$:

$$\Pi_0=-N\nu\lambda(2\lambda-1)^{1/14}\lambda^{-1/7}\nu^{1/28} \times\exp\left[-\frac{2\beta^2I_0(\lambda)}{\sqrt{\nu}}\right]\ , \tag{2.20}$$

$$I_0(\lambda)=\int_0^1dx\frac{(1+x)^{3/4}(1-x)^{1/4}}{1-\beta^2x^2}\ , \tag{2.21}$$

and $N\approx 2.73$ is a constant obtained by the linear theory.

Note that Π_1 and Π_2 oscillate rapidly as $\nu\to 0$ but out of phase. We thus establish that the solvability conditions are not satisfied for $\lambda<\frac{1}{2}$.

(b) $\lambda>\frac{1}{2}$. In this limit the branch cuts run from $\eta=\pm(i/\beta)$ to $\pm i\infty$. Therefore the stationary phase η_+,

which is above (or below for η_-) the branch point, should now be regarded as complex-conjugate pairs and the steepest-descent path runs from $\eta=-\infty$ to $\eta=\eta_+-\delta$ with $\delta\ll 1$, running through the branch point $\eta=i/\beta$ back up to $\eta=\eta_++\delta$, and runs away to $+\infty$. The dominant contribution will come from integrating around the new stationary point η_+ but due to the cut running from η_+ to i/β, one should also include the contribution coming from integrating along this cut. The integration around η_+ produces the exponential factor $S(y_0,\lambda,\nu)$ with an imaginary term:

$$S(y_0,\lambda,\nu)\approx\exp\left[-\frac{2\beta^2}{\sqrt{\nu}}I_0(\lambda)\right]\exp\left[\frac{i2\beta^2 y_0 g(\lambda)}{\sqrt{\nu}}\right], \tag{2.22}$$

where $g(\lambda)$ is given by Eq. (2.21). The integration for $|\Psi(\eta)|$ along the cut from the stationary point $\eta=\eta_+$ to the branch point $\eta=i/\beta$ consists of two parts. First, the discontinuity in $\Psi(\eta)$ along the cut will be approximately of the order of $(2\lambda-1)^{3/4}$ by Eq. (2.18a). Second, the contribution from the pole at $\eta=i/\beta$ can be estimated easily by integrating $\Psi(\eta)$ around the pole, and the result is

$$\pi i\frac{(2\lambda-1)^{3/4}}{1-\lambda}\ . \tag{2.23}$$

Combining all these contributions together, in the limit $\lambda\to\frac{1}{2}$ and $\nu\to 0$, the complex solvability function $\Pi=\Pi_1-i\Pi_2$ can be approximately written as

$$\Pi_1\approx\exp\left[-\frac{2\beta^2}{\sqrt{\nu}}I_0(\lambda)\right]\times\cos\left[\frac{2\beta^2 y_0}{\lambda\sqrt{\nu}}g(\lambda)+C_0\frac{(2\lambda-1)^{3/4}}{\sqrt{\nu}}\right], \tag{2.24a}$$

$$\Pi_2\approx\exp\left[-\frac{2\beta^2}{\sqrt{\nu}}I_0(\lambda)\right]\times\sin\left[\frac{2\beta^2 y_0}{\lambda\sqrt{\nu}}g(\lambda)+C_0\frac{(2\lambda-1)^{3/4}}{\sqrt{\nu}}\right], \tag{2.24b}$$

where C_0 is some constant whose precise value is not important. Note that both Π_1 and Π_2 oscillate rapidly as $\nu\to 0$ but out of phase. Thus the two solvability conditions cannot be satisfied simultaneously and zero-surface-tension solutions disappear in the presence of surface tension. We now turn to the wire perturbation.

III. WIRE PERTURBATION

In Sec. II, it was shown that solvability conditions are not satisfied for asymmetric fingers, which implies, in the language of solvability theory, that a cusp appears at the finger boundary in the presence of surface tension. If one is able to sustain this cusp by the external perturbation, then one should observe asymmetric fingers. In recent experiments performed by Zocchi *et al.* and Rabaud *et al.*, asymmetric fingers were indeed produced when the finger boundaries were perturbed by wires. Four results were reported in their experiments. First, when one wire is placed at the center of the cell, an asymmetric finger with $\lambda<\frac{1}{2}$ develops. Second, when two wires are placed symmetrically along the center of the cell, initially symmetric fingers with $\lambda<\frac{1}{2}$ develop but as the pushing velocity increases λ decreases and then suddenly undergoes a transition to the asymmetric-finger state at the critical finger width λ_c. Third, for given external conditions, the finger width λ appears to be the same as the one obtained by perturbing the tip with a bubble. Fourth, the distance δ between the tip of the asymmetric finger and the wire is a strong function of external parameters, whose functional dependence is unclear though some attempt was made[2] to predict δ as a function of external parameters. In a previous report,[1] a model was proposed to answer the first two questions. It was assumed that the wire creates a negative opening angle at the contact point and the contact angle mainly depends on the tangential slope of the finger profile. This assumption was made by the observation that the contact point is pushed slightly backwards and creates a sharp cusp at the point. In what follows we will briefly describe the main result of Ref. 1. This section is devoted to understanding the remaining two questions in the framework of the solvability theory of pattern selection. We will rederive and thus confirm the previous results and then present new predictions and compare them with the available experimental data.

The starting point of the present analysis is to add to a term on the right-hand side of Eq. (2.6) to represent a cusp produced by external perturbations:

$$\nu\frac{d^2\zeta_1}{d\eta^2}+\nu\frac{d^2\zeta_2}{d\eta^2}+\nu P_1(\eta)\frac{d\zeta_1}{d\eta}+\nu P_2(\eta)\frac{d\zeta_2}{d\eta}+Q(\eta)\zeta_1(\eta)=R(\eta)+\nu\frac{2\beta\lambda}{\pi}\Delta\theta(\eta_0)\delta(\eta-\eta_0)\ . \tag{3.1}$$

Here η is the tangential slope of the zero-surface-tension solution and a cusp appears at $\eta=\eta_0$. The mismatch angle $\Delta\theta(\eta_0)$ is the discontinuity in the tangential slope which is defined as

$$\Delta\theta(\eta_0)=\frac{\left[\frac{d\zeta}{dx}\right]_- -\left[\frac{d\zeta}{dx}\right]_+}{1+\left[\frac{d\zeta_0}{dx}\right]^2}\ , \tag{3.2}$$

where $\zeta(x)$ and $\zeta_0(x)$ are equations for the finger surface with and without surface tension and $+$ and $-$ refer to the limit approaching from left and right, respectively. In Fig. 2 a schematic picture of positive and negative mismatch angle is shown. The additional term on the right-hand side of Eq. (3.1) represents an amount of mismatch angle at $\eta=\eta_0$. Regarding the whole right-hand side as an inhomogeneous term and taking the real and imaginary part of the null eigenvectors, $\zeta_1(\eta)$ and $\zeta_2(\eta)$, to the adjoint operator, one can write down the two solvability conditions Π_1 and Π_2. For $\lambda<\frac{1}{2}$, we have

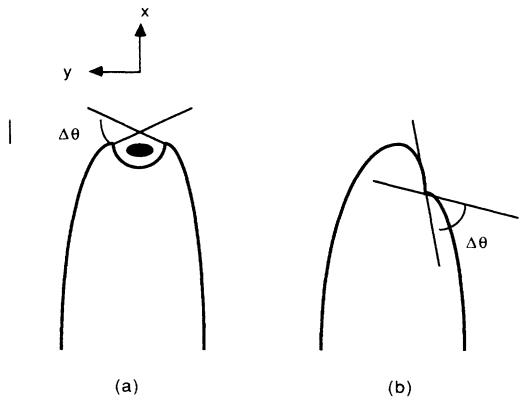

FIG. 2. Schematic pictures of fingers with positive and negative mismatch angles on the finger surface. (a) Positive mismatch angle created by Couder's bubble at the tip. (b) Rabaud *et al.* and Zocchi *et al.*'s negative mismatch angle created by the wire.

$$\Pi_1=\frac{\nu\beta\lambda}{\pi}\frac{(1+\eta_0^2)^{1/2}}{1+\beta^2\eta^2}\Delta\theta(\eta_0)\zeta_1(\eta_0)$$
$$\approx-\Pi_0\cos\left[\frac{2y_0\beta^2 g(\lambda)}{\lambda\sqrt{\nu}}\right], \tag{3.3a}$$
$$\Pi_2=\frac{\nu\beta\lambda}{\pi}\frac{(1+\eta_0^2)^{1/2}}{1+\beta^2\eta_0^2}\Delta\theta(\eta_0)\zeta_2(\eta_0)$$
$$\approx+\Pi_0\sin\left[\frac{2y_0\beta^2 g(\lambda)}{\lambda\sqrt{\nu}}\right], \tag{3.3b}$$

where Π_0 is given by (2.20) and ζ_1,ζ_2 are given by

$$\zeta_1(\eta)=\frac{1+\beta^2\eta^2}{\sqrt{2}\beta}\frac{1}{(1+\eta_0^2)^{1/2}}\cos\left[\frac{2\beta^2}{\sqrt{\nu}}\Psi_1(\eta_0)-\frac{3}{4}\phi\right]$$
$$\times\exp\left[-\frac{2\beta^2}{\sqrt{\nu}}\Psi_2(\eta)\right], \tag{3.4a}$$
$$\zeta_2(\eta)=\zeta_1(\eta)\tan\left[\frac{2\beta^2}{\sqrt{\nu}}\Psi_1(\eta_0)-\frac{3}{4}\phi\right], \tag{3.4b}$$

where

$$\tan\phi=\eta, \tag{3.5a}$$
$$\Psi_1(\eta)=\frac{1}{\sqrt{2}}\int_0^\eta d\eta'\frac{(1+\eta^2)^{1/4}}{1+\beta^2\eta^2}[1+(1+\eta)^{1/2}]^{1/2}, \tag{3.5b}$$
$$\Psi_2(\eta)=\frac{1}{\sqrt{2}}\int_0^\eta d\eta'\frac{(1+\eta^2)^{1/4}}{1+\beta^2\eta^2}[1+(1+\eta)^{1/2}-1]^{1/2}. \tag{3.5c}$$

We now consider two cases.

(a) *Symmetric finger.* $y_0=0$. It is important to reproduce the earlier results of symmetric fingers obtained in Ref. 1. In this case, $\zeta_1(\eta)$ is purely antisymmetric and $\zeta_2(\eta)$ and $R(\eta)$ are purely symmetric. Therefore Π_2 will vanish automatically and $\zeta_2(\eta_0)=0$. Therefore the following condition must be satisfied:

$$\sin\left[\frac{2\beta^2\eta_0}{\sqrt{\nu}}-\frac{3}{4}\phi(\eta_0)\right]=0. \tag{3.6}$$

In the limit of $\nu\to0$ and for the most stable finger with the smallest λ, the solution of the above equation is

$$\frac{2\beta^2}{\sqrt{\nu}}\eta_0\approx\pi. \tag{3.7}$$

Upon performing the integral for Π_1 and using the above relation, we obtain

$$\Delta\theta(\eta_0)=-\exp\left[\frac{\beta^2}{\sqrt{\nu}}\frac{\eta_0^2}{\sqrt{2}}\right]\Delta\theta(0), \tag{3.8}$$

where

$$\Delta\theta(0)=N\lambda^{-1/7}(1-2\lambda)^{1/14}\nu^{1/28}\exp\left[-\frac{2\beta^2}{\sqrt{\nu}}I_0(\lambda)\right]. \tag{3.9}$$

Here $I_0(\lambda)$ is given by (2.21), the multiplicative constant $N\approx2.22$, and $\Delta\theta(0)>0$ is the mismatch angle at the tip which opens up when the correct boundary is imposed at the tail of the finger and the tip is relaxed. Using (3.7), one can easily verify that $\Delta\theta(\eta_0)$ is given by

$$\Delta\theta(\eta_0)\approx-\exp\left[\frac{\pi\eta_0}{4}\right]\exp\left[-\frac{\pi}{\eta_0}I_0(\lambda)\right]. \tag{3.10}$$

Note that $\Delta\theta(\eta_0)$ cannot be greater than 2π. Therefore we expect that our analysis breaks down for large η_0. Since $I_0(\lambda)$ is insensitive to λ except at λ near $\frac{1}{2}$ (see Fig. 3),[13] we thus establish that the mismatch angle $\Delta\theta(\eta_0)$ mainly depends on the slope η_0, which was postulated in Ref. 1 as an attempt to explain the experimental observation made by Zocchi *et al.* They placed two wires symmetrically along the center of the cell and pushed the fluid from the left. Initially, narrow fingers of $\lambda<\frac{1}{2}$, develop and λ decreases as the pushing velocity increases. Then the finger undergoes a sudden transition to an asymmetric finger at a critical finger width. The model

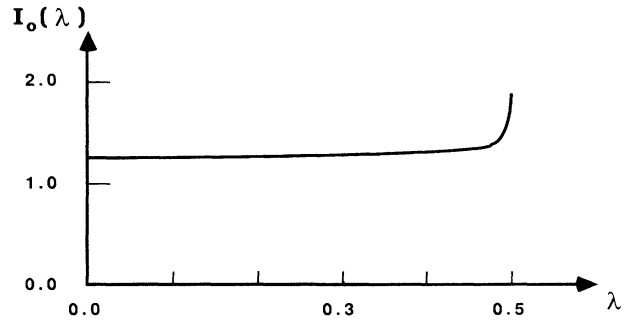

FIG. 3. Values of $I_0(\lambda)$ defined in Eq. (2.10) as a function of λ. Apart from λ close to $\frac{1}{2}$, $I_0(\lambda)$ is insensitive to λ.

proposed in Ref. 1 assumes that as the fluid is pushed, the contact angle made by the wire increases, and that there exists a critical contact angle at the finger surface above which the finger is no longer stable. Even though the assumption about the stability of the finger is debatable and requires a detailed stability analysis, the existence of the maximum contact angle is a quite reasonable assumption. Once this assumption is made the rest of the analysis is straightforward. Since $\Delta\theta(\eta_0)$ mainly depends on η_0 by Eq. (3.11) there should exist η_c in η space where the mismatch angle hits the maximum. η is the tangential slope at the finger boundary. By differentiating Eq. (2.5) for the symmetric finger, one finds that

$$\eta_c = \frac{1-\lambda_c(D)}{\lambda_c(D)} \tan\left[\frac{\pi D}{4\lambda_c(D)}\right], \tag{3.11}$$

where D is the distance between two wires, and $\lambda_c(D)$ is the critical finger width. We set η_c as a free parameter in this paper and fix it by the experimental data of Zocchi *et al.* Zocchi *et al.* placed two wires the distance $D=0.1328$ and observed a transition at $\lambda_c \approx 0.41$. Thus we find $\eta_c \approx 0.374$. Once η_c is determined, (3.12) gives the desired relation between λ_c and D. For example, when $D=0.0944$, Zocchi *et al.* observed a transition at $\lambda_c=0.35$, while (3.2) with $\eta_c=0.374$ predicts $\lambda_c=0.357$. At present, however, there are not sufficient data to check (3.11). We now turn our attention to the asymmetric case.

(b) *Asymmetric case.* We consider the case $y_0 \neq 0$ with the mismatch angle opening up at the center of the cell. This case will describe the experimental situation where one wire is placed at the center of the cell: $y=0$. One can easily find the tangential slope at $y=0$ by Eq. (2.5),

$$\eta_0 = \frac{(1-\lambda)}{\lambda} \tan\left[\frac{\pi y_0}{2\lambda}\right]. \tag{3.12}$$

Substituting Eq. (3.12) into Eq. (3.3) and using (2.19) for Π_1 and Π_2, one obtains the following two solvability conditions for $\lambda < \frac{1}{2}$, the central result of this paper:

$$\tan\left[\frac{\pi y_0}{\sqrt{\nu}(1-\lambda)}\right] \approx -\tan\left[\frac{2\beta^2 y_0 g(\lambda)}{\sqrt{\nu}}\right], \tag{3.13a}$$

$$\Delta\theta(y=0,y_0)\cos\left[\frac{\pi y_0}{\sqrt{\nu}(1-\lambda)}\right] \approx \Delta\theta(y=0,y_0=0)\cos\left[\frac{2\beta^2 y_0 g(\lambda)}{\sqrt{\nu}}\right], \tag{3.13b}$$

(3.13a) was obtained by dividing both sides of (3.3a) and (3.3b), and (3.13b) was obtained from (3.3a) by using (2.19) and (3.9). As we will see, the above two solvability conditions contain all the relevant information for the wire experiments. From (3.13a) and (3.12), we find

$$\frac{\pi y_0}{\sqrt{\nu}(1-\lambda)} \equiv \frac{y_0}{\sqrt{B}} = \pi - \frac{2y_0\beta^2 g(\lambda)}{\lambda\sqrt{\nu}} \equiv \pi - \frac{2\lambda g(\lambda)}{\pi(1-\lambda)} \frac{y_0}{\sqrt{B}}, \tag{3.14}$$

where we define B, the new experimentally measurable variables, as

$$B = \frac{(1-\lambda)^2}{\pi}\nu. \tag{3.15}$$

Note that when (3.14) is satisfied, the angle $\Delta\theta(y_0,y=0)$ becomes *negative.* This explains why one never observes a symmetric finger with wire at the center because the mismatch angle for the symmetric finger at the tip is always *positive.* Moreover, (3.13b) says *the absolute magnitude of the mismatch angle created by the wire for nonzero y_0 is precisely the same as the one which opens at the tip for the symmetric finger.* In what follows we show how this explains the experimental observation made by Rabaud *et al.* that the finger width with one wire at the center appears to be the same as those obtained by the bubble. Since $\Delta\theta(y_0=0,y=0)$ is a function of both λ and B, for fixed mismatch angle, the above equation and (3.14) produce relations between B, y_0, and λ. The mismatch angle is determined by the experimental conditions at the contact point and in general we do not know the precise value. However, in comparison to the experiment, the precise knowledge of $\Delta\theta$ is not important. First, the mismatch angle $\Delta\theta$ is not the same as the contact angle and is unobservable. Second, λ and y_0 logarithmically depend on $\Delta\theta(y_0=0,y=0)$ for a given B, by (3.9); thus one can safely assume $\Delta\theta(y_0=0,y=0)$ as a constant if it does not change dramatically. The precise prediction of (3.13b) becomes clear when we display $\Delta\theta$ in terms of external parameters. We find the same result as was obtained in Ref. 4. [See Eqs. (3.4) and (3.5) of Ref. 4.] The present linear theory predicts that the finger width obtained by the wire perturbation should be precisely the same as the one obtained by the bubble perturbation for the symmetric finger at the tip. The correction is at least second order in y_0 and is negligible in the linear approximation.[14] This explains the experimental observation of Rabaud *et al. They perturbed the finger by the wire and found that for given B, the finger thickness is the same as the one obtained by the bubble perturbation.*

Here we are establishing that all the experimental results obtained by the bubble perturbation can be carried over to the one wire experiment in the limit $y_0 \ll 1$. Examples are: (1) if the external parameters are kept constant and only the wall size is allowed to change, we would expect the same result as the one obtained by the bubble perturbations. (2) Dependence of the tip radius as well as the finger width on the external parameters for

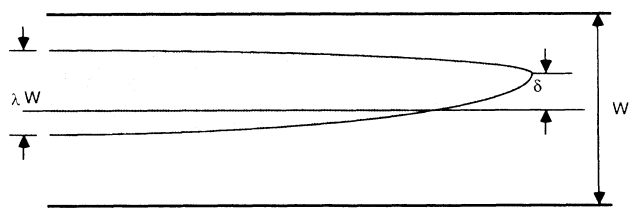

FIG. 4. Distance δ from the tip of the finger to the wire at the center.

TABLE I. Comparison between the theoretical prediction (3.16) and the experiments of Rabaud *et al.* and Zocchi *et al.*

λ	$g(\lambda)$
0.1	1.0496
0.2	1.0629
0.3	1.0983
0.4	1.1987
0.45	1.3371

the asymmetric finger is also the same. (3) With one wire in a *radial* Hele-Shaw cell, we will obtain the same prediction as in the bubble experiment: The dimensionless group

$$\sigma=\frac{\gamma\kappa^2 b^2}{12\mu U}$$

is selected, in the limit $U\to 0$, at

$$\sigma^*\approx 0.379/[\ln(\Delta\theta)]^2$$

[Eq. (3.9) of Ref. 4]. What is not clear at present, however, is whether the above results apply equally well to the experiment with one wire at any point. Rabaud informed us that the lateral wall does not seem to have any effect on his result, indicating that the position of the wire is not important.

We now compare another prediction, Eq. (3.14), with the experimental results of Zocchi *et al.* and Rabaud *et al.* They measured the distance between the tip of the asymmetric finger and the wire. Note that this distance is *not* y_0. Let this distance be δ. (See Fig. 4.) Then δ will be the distance between the tip of the asymmetric finger and the center of the cell $y=0$. By differentiating Eq. (2.5) one can locate the tip and find

$$\delta\approx\left[1+\frac{2\lambda}{\pi(1-\lambda)}\right]y_0$$

$$\approx\pi\left[1+\frac{1}{\pi}\frac{2\lambda}{(1-\lambda)}\right]\sqrt{B}\Big/\left[1+\frac{1}{\pi}\frac{2\lambda}{(1-\lambda)}g(\lambda)\right], \quad (3.16)$$

where $g(\lambda)$ is given by Eq. (2.18c) and Eq. (3.14) is used to obtain the final relation. The value for $g(\lambda)$ is given in Table I. Note that in the above equation, there are *no adjustable parameters.* All the parameters that enter (3.16) are the experimentally measurable quantities. In Table II are shown theoretical predictions and the experimental results of Zocchi *et al.* and Rabaud *et al.* The agreement with the experiment seems to be fairly good, given the fact that the error bars in the data are quite big. More precise experimental data are needed to check (3.16).

TABLE II. Values of $g(\lambda)$ for different values of λ.

$1/B$	$1/\lambda$	δ (expt.)	δ (predicted)
2500	0.4	0.09–0.13	0.097
6110	0.345	0.067–0.042	0.0388
17 280	0.3	0.040	0.0234

In summary, we have considered the selection mechanism of *asymmetric* Saffman-Taylor fingers and derived *not one but two* solvability conditions. Surface tension is not enough to break the two-parameter continuous family of solutions, characterized by the dimensionless width of the finger λ and y_0 the degree of asymmetry. A concave cusp appears on the finger boundary in the presence of surface tension. For $y_0\ll 1$, the magnitude of this concave cusp is, within linear approximation, precisely the same as the one which opens at the tip of the symmetric fingers. Therefore all the results obtained in the bubble experiment should be carried over to one wire experiment at the center. We then showed how the recent wire experiments of Zocchi *et al.* and Rabaud *et al.* may be understood from the viewpoint of the solvability theory of pattern selection by assuming that the perturbation caused by the wire is effectively equivalent to opening a concave cusp at the contact point. We found fair agreement with the theoretical predictions and the available data.

Note added in proof. The author has recently learned that Shaw[15] obtained a similar result for the asymmetry parameter y_0 in the presence of wire perturbation. If we set $g(\lambda)=1$ in (3.14), it reduces to his result.

ACKNOWLEDGMENTS

I wish to thank G. Zocchi for many helpful discussions on his experimental results. I also wish to thank M. Rabaud for sending his experimental data prior to publication as well as Professor S. Tanveer for sending a copy of his work prior to publication. I also wish to thank Professor F. Family for helpful comments on the manuscript, Dan Platt for numerical assistance, and Irene Kim for a careful reading of the manuscript. This research was supported by the U.S. Office of Naval Research and the Petroleum Research Fund administered by the American Chemical Society.

*Permanent address.

[1]D. C. Hong, Phys. Rev. A **37**, 2724 (1988).

[2]G. Zocchi, B. Shaw, A. Libchaber, and L. Kadanoff, Phys. Rev. A **35**, 1894 (1987); M. Rabaud, Y. Couder, N. Gerard, *ibid.* **37**, 935 (1988).

[3]Y. Couder, N. Gerard, and M. Rabaud, Phys. Rev. A **34**, 5175 (1986).

[4]D. C. Hong and J. S. Langer, Phys. Rev. A **36**, 2325 (1987).

[5]P. G. Saffman and G. I. Taylor, Proc. R. Soc. London, Ser. A **245**, 312 (1958). There appeared several review articles recently. See G. M. Homsey, Annu. Rev. Fluid Mech. **19**, 271 (1987); P. G. Saffman, J. Fluid. Mech. **173**, 73 (1986); D. Besimon, L. Kadanoff, S. Liang, B. Shraiman, and C. Tang, Rev. Mod. Phys. **58**, 977 (1986), and references therein.

[6]Y. Couder, O. Cardoso, D. Dupuny, P. Tanveriner, and W. Thom, Europhys. Lett. **2**, 437 (1986); Y. Couder, N. Gerard,

and M. Rabaud, Phys. Rev. A **34**, 5175 (1987).

[7]D. Bensimon, Phys. Rev. A **33**, 1302 (1986); D. Kessler and H. Levine, *ibid.* **33**, 2621 (1986); **33**, 2634 (1986).

[8]G. I. Taylor and P. G. Saffman, Q. J. Mech. Appl. Math. **12**, 265 (1959).

[9]B. I. Shraiman, Phys. Rev. Lett. **56**, 2028 (1986); D. C. Hong and J. S. Langer, *ibid.* **56**, 2032 (1986); R. Combescot, T. Dombre, V. Hakim, Y. Pomeau, and A. Pumir, *ibid.* **56**, 2036 (1986).

[10]Excellent review articles on this subject are now available. See J. S. Langer, in *Chance and Matter,* Proceedings of the Les Houches Summer School, Session 46, edited by J. Souletie, J. Vannimenus, and R. Stora (North-Holland, Amsterdam, 1986); D. Kessler, J. Koplik, and H. Levine, Adv. Phys. (to be published).

[11]S. Tanveer (unpublished).

[12]A. Barbieri, D. C. Hong and J. S. Langer, Phys. Rev. A **35**, 1802 (1987).

[13]I wish to thank M. Rabaud who kindly provided this figure.

[14]The nonlinear analysis along the line of Kruskal and Segur (unpublished) will not change the essential result of this paper. The reason is that the mismatch angle derived by (3.1) is proportional to the solvability function Π, for which the nonlinear analysis produces the same form except for the multiplicative constant N.

[15]Bruce Shaw, Proceedings of the Statistical Mechanical Meeting, Rutgers University, Piscataway, NJ, December, 1988 (unpublished).